Int. J. Heat Mass Transfer. Vol. 27, No. 10, pp. 1771–1779, 1984
Printed in Great Britain

0017 9310/84 $3.00 + 0.00
Pergamon Press Ltd.

Heat transfer and flow around an elliptic cylinder

TERUKAZU OTA, HIDEYA NISHIYAMA
Department of Mechanical and Production Engineering, Akita University, Akita 010, Japan

and

YUKIYASU TAOKA
Nippon Kokan Corp. Ltd., Yokohama 230, Japan

(*Received* 17 *November* 1983)

Abstract—Heat transfer characteristics and flow behaviors have been made clear for an elliptic cylinder of axis ratio 1 : 3. The testing fluid was air and the Reynolds number ranged from about 8000 to 79 000. The angle of attack α was varied from 0° to 90°. The local and overall heat transfer features are clarified in relation to the flow behaviors around the cylinder. The critical Reynolds number is detected, where the heat transfer and flow characteristics change drastically. It is found that the mean heat transfer coefficient is at its highest at $\alpha = 60°$–90° over the whole Reynolds number range studied and also that even the lowest value of the mean heat transfer rate is still higher than that for a circular cylinder. Effects of the axis ratio of the elliptic cylinder are also discussed in comparison with previous works.

1. INTRODUCTION

THE EXPLOITATIONS of high performance heat exchangers for saving and making effective use of energy is a very important and urgent problem. Among many types of heat exchangers, those constructed of circular pipes have been used in many industries. Flow around pipes, however, is not necessarily normal to the pipe axis. In such a situation, the cross-section of a pipe in the flow direction becomes an ellipse. An elliptic cylinder is a basic and general form, which becomes a flat plate and also a circular cylinder depending on the axis ratio. There have been many works on the flow around elliptic cylinders [1–7] and the flow characteristics are found to change considerably with axis ratio and also angle of attack [4–7]. Furthermore, their drag coefficient at a small angle of attack is lower than that of a circular cylinder. This may be an advantageous feature when using elliptic tubes as a heat transfer surface element, since the pumping power needed to flow fluids around them may become very small.

As far as forced convection heat transfer characteristics of the elliptic cylinder are concerned, there have been only a few investigations. Eckert [8] and Chao and Fagbenle [9] made boundary layer analyses. Their results, naturally, may be applicable only to the upstream surface of the elliptic cylinder on which a laminar boundary layer develops. Seban and Drake [10] and Drake *et al.* [11] measured the local heat transfer coefficient on elliptic cylinders of axis ratio 1 : 4 and 1 : 3, respectively. Their main purpose, however, seems to consist of confirming an applicability of the boundary layer theory. The angle of attack examined by them was limited to 0°, 5° and 6°, and the mean heat transfer coefficient was not measured. Reiher [12] reported the mean heat transfer coefficient for an elliptic cylinder at 0° and 90°, but its configuration was obscure. On the other hand, it is reasonable to consider that the heat transfer characteristics of the elliptic cylinder vary remarkably with the angle of attack, since the flow features change greatly, as previously noted.

From this standpoint, the present authors have conducted an experimental study of forced convection heat transfer from an elliptic cylinder of axis ratio 1 : 2 [13]. The local heat transfer features are clarified and it is found that they are quite different from those of the circular cylinder. The mean heat transfer coefficient depends upon the angle of attack along with the Reynolds number and it is higher than that from the circular cylinder at all angles of attack over the Reynolds number range studied. The flow features around the elliptic cylinder, however, change with its axis ratio. In accordance with such a change of the flow, the heat transfer characteristics inevitably vary with the axis ratio of the elliptic cylinder.

The purpose of the present study is to investigate the local and overall heat transfer characteristics from an elliptic cylinder of axis ratio 1 : 3. The angle of attack is varied from 0° to 90° and the variation of the heat transfer feature with it is discussed in relation to the flow behaviors around the cylinder. Furthermore, effects of the axis ratio of the cylinder upon the overall heat transfer rate are discussed in comparison with previous results for a circular cylinder [14] and also for an elliptic cylinder of axis ratio 1 : 2 [13].

NOMENCLATURE

$2a$ or c	length of major axis of elliptic cylinder
$2b$	length of minor axis of elliptic cylinder
C_D	pressure drag coefficient
C_p	static pressure coefficient, $(P-P_\infty)/\frac{1}{2}\rho U_\infty^2$
d	diameter of circular cylinder of equal circumferential length
h	local heat transfer coefficient, $q/(T_w-T_\infty)$
h_m	mean heat transfer coefficient
Nu	local Nusselt number, hc/λ
Nu_m	mean Nusselt number, $h_m c/\lambda$
Nu_{md}	mean Nusselt number, $h_m d/\lambda$
P	static pressure
q	heat flux per unit area and unit time
Re	Reynolds number, $U_\infty c/\nu$
Re_d	Reynolds number, $U_\infty d/\nu$
s	surface length from leading edge
St	Strouhal number, fc/U_∞
T	temperature
U, u	streamwise mean and turbulent fluctuating velocities
W	wake width
x	distance from cylinder axis in direction of upstream uniform flow
y	distance normal to x-axis.

Greek symbols

α	angle of attack
λ, ν, ρ	thermal conductivity, kinematic viscosity and density of air at T_∞, respectively.

Subscripts

d	based on d as reference length
w	wall.

2. EXPERIMENTAL APPARATUS AND TECHNIQUE

The wind tunnel used in the present study is the same as that employed in previous works by the authors [15, 16], though a circular test section of 254 mm in diameter and 605 mm long was installed. Two side plates of 10 mm thick Plexiglas were equipped in the test section in order to ensure the two-dimensionality of the flow, their spanwise distance being 150 mm.

The test elliptic cylinder had an axis ratio of 1 : 3, its major axis length being 50 mm and its spanwise length being 150 mm. It was made of fiber-reinforced plastics by the same procedure as in the previous work [13]. Heating of the cylinder was conducted by means of an electric current to a 0.05 mm thick, 29 mm wide stainless steel sheet, which was wound helically and stuck onto the cylinder surface. Forty-one copper–constantan thermocouples 0.07 mm in diameter were embedded on the cylinder surface in order to measure the wall temperature. Heat loss by conduction and radiation was neglected in the following results.

The experiments were conducted under the condition of constant heat flux. The upstream uniform flow velocity U_∞ ranged from about 2 to 22 m s^{-1} and the corresponding Reynolds number $Re = U_\infty c/\nu$ from about 8000 to 79 000. The free stream turbulence intensity $\sqrt{u^2}/U_\infty$ was about 0.007 in the above velocity range. The angle of attack α was varied from 0° to 90° in order to clarify variations of the heat transfer characteristics of the cylinder with it. In the present paper, α denotes an inclination angle of the major axis of the elliptic cylinder to the direction of the upstream uniform flow. The mean and turbulent fluctuating velocities in the near wake were measured with a constant temperature hot-wire anemometer with a linearizing circuit. An FFT analyzer was also used to detect a vortex shedding frequency from output voltages of the anemometer.

Furthermore, another elliptic cylinder was made and used in measuring the static pressure distribution along the cylinder surface in order to make clearer correlations between the heat transfer and the flow characteristics. The wind tunnel used was the same as in our previous work [17], the test section of which was 150 mm wide, 500 mm high and 800 mm long. The test elliptic cylinder was almost the same as in the heat transfer study, say the major axis length 50 mm and the spanwise one 150 mm. However, its surface was not covered with a stainless steel sheet but had 30 pressure holes 0.3 mm in diameter. With the intention of minimizing mutual interferences of the pressure holes, they were drilled helically on the surface.

The tunnel blockage ratio varied from 0.07 at $\alpha = 0°$ to 0.20 at $\alpha = 90°$ in the heat transfer study. That in the measurements of the static pressure ranged from 0.03 at $\alpha = 0°$ to 0.10 at $\alpha = 90°$. In the present paper, however, no corrections were made for the tunnel wall effects upon the heat transfer and flow characteristics. In the preliminary experiments, effects of the heat flux q were found to be negligible and the position of $\alpha = 0°$ was determined with detailed measurements of the local heat transfer and pressure coefficients on the upper and lower sides of the cylinder at various Reynolds numbers.

3. EXPERIMENTAL RESULTS AND DISCUSSION

3.1. *Heat transfer characteristics*

Local heat transfer distributions around the whole circumference of the elliptic cylinder are represented for

$\alpha = 0°$–$90°$ at various Reynolds numbers in Figs. 1–4.

Figure 1 shows the results at $\alpha = 0°$, which include previous theoretical and experimental results for comparison [11, 13]. It is clear that the symmetry of the local heat transfer distribution on the upper and lower surfaces is satisfactory at all the Reynolds numbers. In the following, the positive value of s is located on the upper surface of the cylinder. It may be reasonable to consider that the whole Reynolds number range tested is included within the subcritical flow region, since the heat transfer distribution shows no essential change with Reynolds number. Therefore, the present data are demonstrated in the form of $Nu/\sqrt{Re}$, and they fall into a single curve on the upstream surface. It implies that a laminar boundary layer develops on the upstream surface of the cylinder and the local heat transfer rate is proportional to the square root of the Reynolds number, as the boundary layer theory suggests [9, 11]. However, the flow separates at about $s/c = \pm 0.7$, which is located a little downstream of the minor axis of the cylinder, and a dependency of $Nu/\sqrt{Re}$ upon Re can be recognized in the separated flow region. That is, the flow therein is very complicated and may not be regarded as laminar. It is clear in the figure that the present data agree with the theoretical data of Drake *et al.* [11] rather than that of Chao and Fagbenle [9], who treated an elliptic cylinder of axis ratio 1:2.96 by Schubauer [1]. Data of Drake *et al.* were obtained at $Re = 960\,000$. The difference between the present data and theirs may originate from compressibility effects of fluid and an accuracy of the elliptic cylinder, especially of the leading edge, may also be a factor.

Represented in Fig. 2 are the results at $\alpha = 15°$. It is very clear that the local heat transfer distribution changes drastically at about $Re = 44\,000$. That is, Nu shows a maximum near the leading edge and steeply decreases on both sides of the cylinder with increasing the surface distance. On the lower (or the pressure) side, Nu reaches a minimum at about $s/c = -0.9$

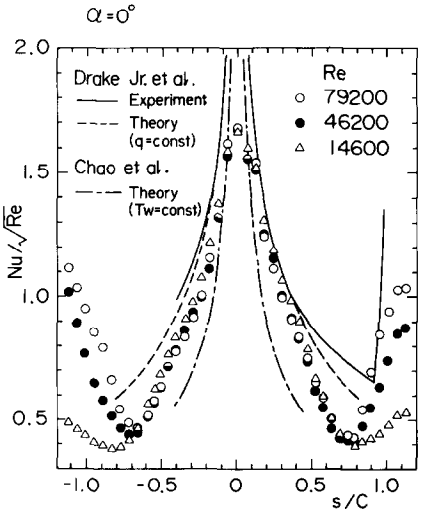

FIG. 1. Local Nusselt number distribution.

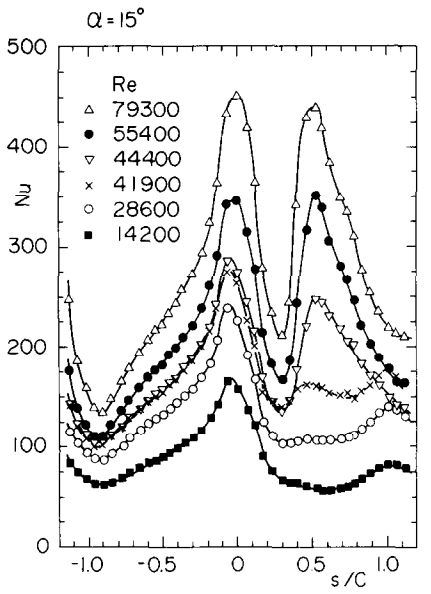

FIG. 2. Local Nusselt number distribution.

independently of the Reynolds number. However, on the upper (or the suction) side, at Reynolds numbers greater than about 44 000, Nu becomes a minimum at $s/c = 0.3$. Then it increases rapidly, reaches a maximum at about $s/c = 0.5$ whose value is nearly equal to the maximum near the leading edge and subsequently decreases again to the downstream. Such a characteristic variation of the local Nusselt number may be originated from a generation of the so-called separation bubble [18, 19], whose existence was confirmed with the surface oil flow pattern. That is, a laminar boundary layer separates at $s/c = 0.3$, a separated shear layer transits to a turbulent one, which subsequently is reattached onto the cylinder surface at about $s/c = 0.5$. After that a turbulent boundary layer develops in the neighborhood of the trailing edge without separation. Similar variation of the flow and heat transfer features is observed for a circular cylinder at the critical Reynolds number [20]. Therefore, in the present study on the elliptic cylinder, the critical Reynolds number Re_c exists, at which the flow and heat transfer characteristics vary drastically. It is found that the critical Reynolds number changes with the angle of attack. Its value is a minimum around $\alpha = 10°$ and increases at both lower and higher values of α. Variations of the flow around the cylinder at the critical Reynolds number are represented in the following. On the other hand, at a Reynolds number lower than Re_c, the laminar boundary layer separates at about $s/c = 0.2$–0.3 and the heat transfer rate in the separated flow region is quite low.

Figure 3 shows the results at $\alpha = 30°$. Nu attains a maximum at about $s/c = -0.05$ and its characteristic feature in the separated flow region is very similar to that for $\alpha = 15°$ in the subcritical flow regime. An increase of the angle of attack brings on a decrease of the

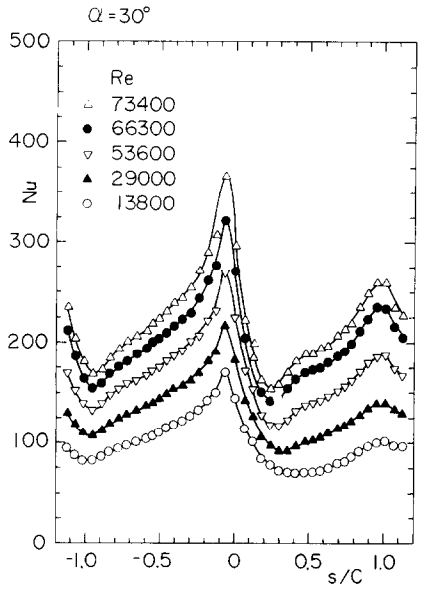

FIG. 3. Local Nusselt number distribution.

flow velocity oncoming to the upstream surface of the cylinder. Furthermore, the wake width is relatively small and then, in the separated flow region, a transversal motion of the fluid may be suppressed. It results in a low heat transfer rate on the whole circumference of the cylinder. Such a behavior of the local heat transfer brings about a low value of the mean heat transfer coefficient at $\alpha = 30°$ over the whole Reynolds number range examined, as de.nonstrated later.

Represented in Fig. 4 are the results at $\alpha = 90°$. It is very interesting to note that Nu is a minimum at the upstream stagnation point (say $s/c = -0.35$), and

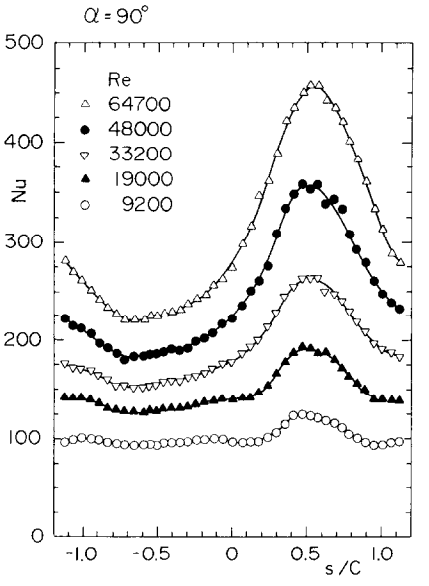

FIG. 4. Local Nusselt number distribution.

increases with the surface distance because of an acceleration of the flow outside the boundary layer. The laminar boundary layer developing on the upstream surface may be regarded to separate in the neighborhood of the leading and trailing edges. Even under such a flow situation, the local heat transfer coefficient shows no minimum around the separation point. Nu furthermore increases with the surface distance and reaches a maximum at the downstream stagnation point. An angle of attack of 90° brings about a much wider wake behind the cylinder and the transversal motion of the fluid is very violent therein. Consequently the cylinder surface is washed out frequently by the fluid entrained from the main flow. It may result in a very large value of Nu as shown in the figure.

These results on the local heat transfer for the elliptic cylinder may suggest that it is very difficult to estimate the flow feature from only the local heat transfer one, e.g. the position of the flow separation.

Figures 5 and 6 show typical examples of a variation of the mean Nusselt number with the Reynolds number. Represented in Fig. 5 are the results at $\alpha = 0°$. It is clear that Nu_m increases almost linearly with Re in logarithmic scale, and an empirical formula obtained with the method of least squares is included in the figure. In general, Nu_m is expressed in the form

$$Nu_m = A\,Re^n. \tag{1}$$

Values of n and A change naturally with the angle of attack and are summarized in Table 1. Data scatter at other angles of attack is of the same order as that at $\alpha = 0°$ in Fig. 5.

On the other hand, in the case of $\alpha = 15°$ shown in Fig. 6, the critical Reynolds number exists and the local heat transfer feature changes drastically there, as described above. Therefore, Nu_m also changes at Re_c and two empirical formulae are obtained depending on the subcritical or the supercritical Reynolds number region, as included in Fig. 6. An increasing rate of Nu_m with Re is large in the supercritical flow regime, since the separation bubble originates and the turbulent boundary layer develops on the downstream surface of the cylinder.

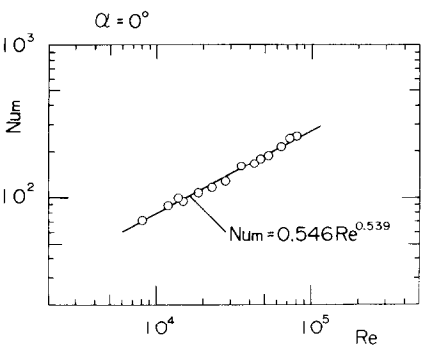

FIG. 5. Mean Nusselt number.

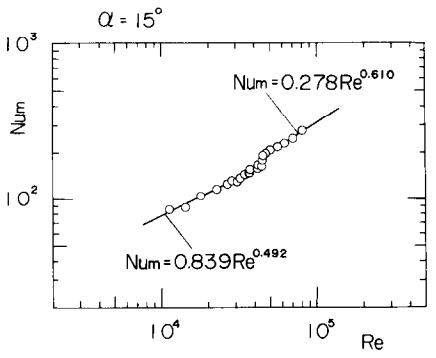

FIG. 6. Mean Nusselt number.

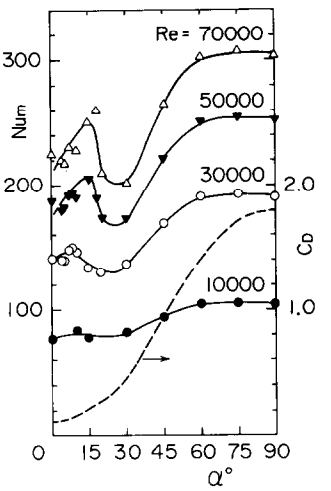

FIG. 7. Variations of mean Nusselt number and pressure drag coefficient with angle of attack: — — —, C_D (Re = 48 000).

It is very interesting and important to investigate a variation of Nu_m with α, since the flow and local heat transfer characteristics change with the angle of attack, as already demonstrated. Figure 7 shows such results. It is clear that Nu_m does not increase monotonically with α. In the low Reynolds number region of $Re < 10\,000$, Nu_m shows no essential change in the region of $\alpha = 0°$–$30°$. Beyond $\alpha = 30°$, it increases with α and again shows no essential variation from $\alpha = 60°$ to $90°$. On the other hand, in the region of $Re > 30\,000$, as α increases from $0°$, Nu_m first increases and reaches a maximum around $\alpha = 10°$–$15°$. Then it decreases and attains a minimum at about $\alpha = 20°$–$30°$. Subsequently it increases once again and finally shows no essential change in the region of $\alpha > 60°$, where Nu_m becomes a maximum over the whole Reynolds number range studied. As described previously in relation to the results at $\alpha = 30°$, in the region of $\alpha = 20°$–$30°$, a decrease of the oncoming flow velocity to the upstream surface of the cylinder brings about a relatively low value of Nu therein. Furthermore, in the separated flow region, Nu is not so high since the transversal motion of fluid may not be so severe as in the case of $\alpha > 45°$. These facts may result in the lowest value of Nu_m at $\alpha = 20°$–$30°$.

To estimate the heat transfer capability of the elliptic cylinder compared to that of cylinders of various cross-sections, it is important to select an appropriate reference length in both Nusselt and Reynolds numbers. It is reasonable to regard the circular cylinder as the most basic and frequently used configuration in engineering. Accordingly selected in the present study is a diameter d of an equivalent circular cylinder, whose circumferential length is equal to that of the present elliptic cylinder. d can be calculated by

$$d = (2E'/\pi)c$$

where $E'(k)$ is an associated complete elliptic integral of the second kind and $k^2 = 1-(b/a)^2$. Accordingly the empirical formula equation (1) can be transformed into

$$Nu_{md} = A' Re_d^n. \tag{2}$$

Values of A' are represented in Table 1.

All the results are summarized in Fig. 8, in which the data points are omitted for clearness and their scatter is of the same order as in Figs. 5 and 6. Reiher's result at $\alpha = 0°$ is included for reference but the exact configuration of his elliptic cylinder is obscure. On the other hand, there have been published so many data on the circular cylinder but their mutual difference is not

Table 1. Effect of angle of attack on n, A and A'.

α (deg.)	n	A	A'
0	0.539	0.546	0.466
15*	0.492	0.839	0.705
15†	0.610	0.278	0.243
30	0.461	1.178	0.979
45	0.532	0.700	0.596
60	0.546	0.684	0.585
75	0.549	0.671	0.575
90	0.548	0.671	0.574

* $8000 < Re < 44\,000$ or $5700 < Re_d < 31\,200$.
† $44\,000 < Re < 79\,000$ or $31\,200 < Re_d < 56\,000$.

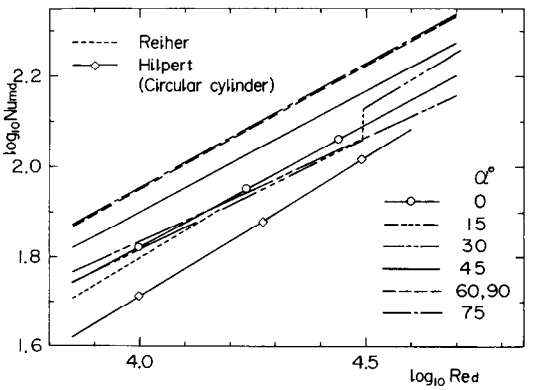

FIG. 8. Effect of angle of attack on mean Nusselt number and comparison with previous data.

small [21]. In this study, a well-known empirical formula by Hilpert [14] in the region of $4000 < Re_d < 40000$ is referred to as a typical one. A correlation proposed recently by Morgan [21] is almost equal to that of Hilpert in the same range.

The present data at $\alpha = 0°$ are in relatively good agreement with that of Reiher but not at $\alpha = 90°$, though his results at $\alpha = 90°$ are omitted. In the low Reynolds number region, the results at $\alpha = 0°$–$30°$ are almost equal to each other. In the high Reynolds number region beyond the critical one, however, Nu_{md} at $\alpha = 30°$ is the lowest. On the other hand, Nu_{md} at $\alpha = 60°$–$90°$ is in good agreement and is the highest over the whole Reynolds number range examined in the present work. It is clear that all the results of Nu_{md} for the present elliptic cylinder, even the lowest one, are higher than those of Hilpert. In accordance with these facts, as far as the heat transfer capability is concerned, the elliptic cylinder of axis ratio 1 : 3 studied is superior to the circular cylinder.

The flow and heat transfer characteristics of the elliptic cylinder varies with its axis ratio b/a. Though there has been little information on the overall heat transfer rate of the elliptic cylinder, an attempt is made to investigate effects of the axis ratio on it referring to the previous data on the elliptic cylinder of axis ratio 1 : 2 by the authors [13] and also those on the circular cylinder by Hilpert noted above. Figure 9 shows representative examples. Nu_{md} of the elliptic cylinder varies with both Re_d and α. It is clear that in general, Nu_{md} increases with an increase of the ratio a/b, at least, in the region of $1 \leqslant a/b \leqslant 3$ but an increasing rate of Nu_{md} from $a/b = 2$ to 3 is smaller than from $a/b = 1$ to 2. However, it is to be noticed that the difference of published data on the circular cylinder is relatively large as described above.

3.2. *Flow characteristics*

Representative examples of the static pressure distribution along the cylinder surface are demonstrated in Fig. 10, which shows the case of $Re = 48000$ included in the subcritical flow regime. Needless to say, the pressure distribution varies with the angle of attack. That is, the upstream stagnation point shifts downstream from the leading edge at $\alpha = 0°$ to the minor axis at $\alpha = 90°$, and the base pressure decreases with an increase of α. It can be detected that at large angles of attack such as 60° and 90°, the upstream separation point almost coincides with the leading edge and the pressure inside the separated flow region is very low. Such a low pressure and a large wake downstream of the cylinder may bring about a violent motion of fluid therein and it results in a very high heat transfer rate as demonstrated previously.

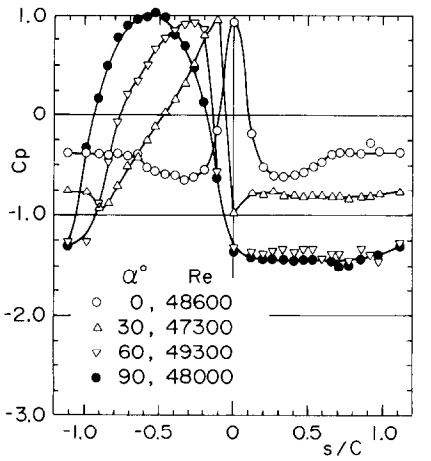

FIG. 10. Pressure distribution.

Figure 11 shows the results at $\alpha = 15°$. At low Reynolds numbers, the flow separates in the laminar state at about $s/c = 0.2$ on the upper surface and the pressure inside the separated flow region is constant, in essence. However, over the critical Reynolds number, a laminar boundary layer separates at about $s/c = 0.3$, reattaches onto the surface at about $s/c = 0.5$ and

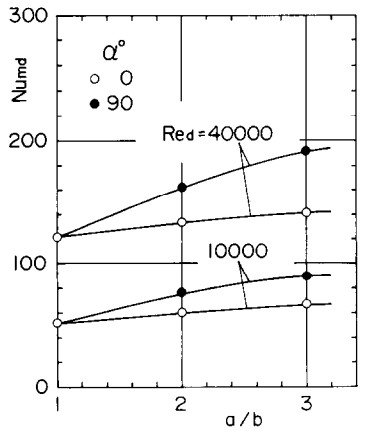

FIG. 9. Variation of mean Nusselt number with axis ratio. Data at $a/b = 1$ by Hilpert.

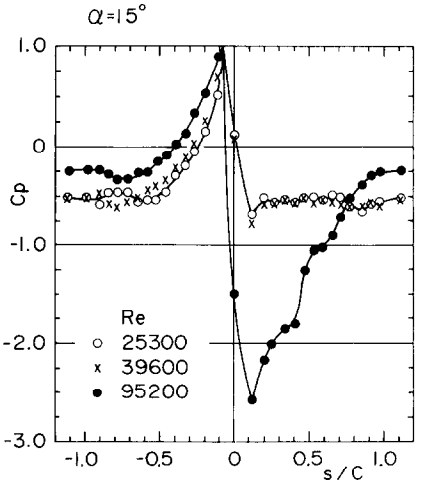

FIG. 11. Pressure distribution.

subsequently a turbulent boundary layer develops downstream. Finally the flow separates at about $s/c = 1.0$ forming a very narrow wake compared to that at the subcritical Reynolds number. Such a feature of the pressure distribution around the surface corresponds well to that of the local heat transfer distribution as represented in Fig. 2.

The pressure drag coefficient C_D is determined numerically from those pressure distributions. Inserted into Fig. 7 is a typical example of a variation of C_D with α at a subcritical Reynolds number, say about $Re = 48\,000$. It is to be noted that the present value of C_D is based upon the major axis length c as the reference length. C_D is about 0.12 at $\alpha = 0°$, increases almost monotonically with α and finally reaches 1.8 at $\alpha = 90°$. In the supercritical Reynolds number region, as α increases from 0°, C_D decreases gradually and reaches a minimum of about 0.05 around 15°. Subsequently it increases discontinuously to a value at the subcritical Reynolds number, though such results in the supercritical flow regime are not shown in Fig. 7 for clarity.

Furthermore, in order to clarify the correlation between the flow and heat transfer features around the elliptic cylinder, the streamwise mean and turbulent fluctuating velocities were measured in the near wake at $\alpha = 15°$, and the results are shown in Fig. 12. The corresponding wake width W and also the Strouhal number St are exhibited in Fig. 13. As described previously, over the critical Reynolds number, on the upper surface of the cylinder, the laminar boundary layer transits to the turbulent one and the separation point shifts far downstream compared to that at the subcritical Reynolds number. Accordingly the wake formed behind the cylinder is very narrow, as clearly shown in Figs. 12 and 13. In the present paper, the wake width is defined as a distance between points of

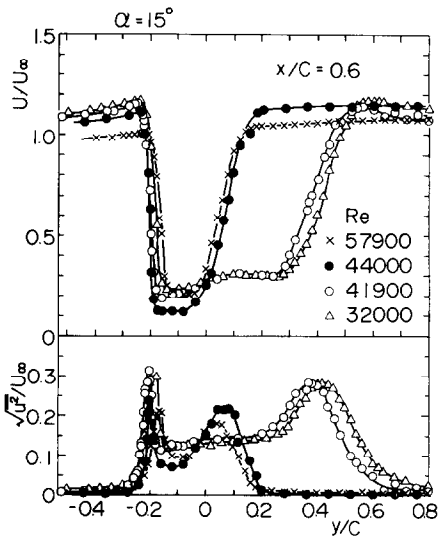

FIG. 12. Streamwise mean and turbulent fluctuating velocities in near wake.

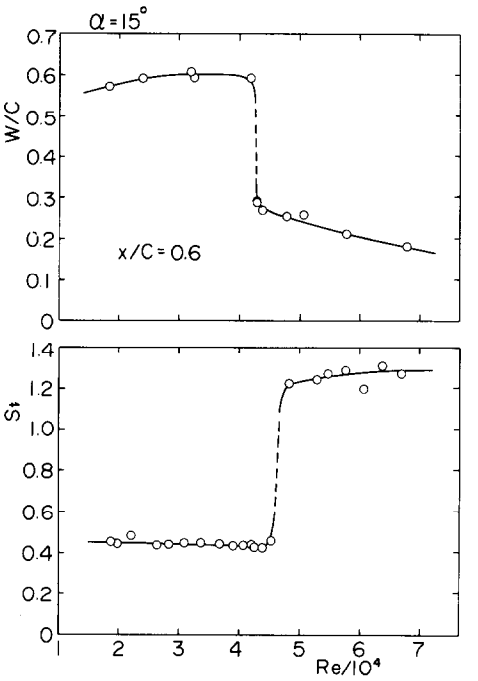

FIG. 13. Wake width and Strouhal number.

maximum turbulence intensity. The Strouhal number increases discontinuously at the critical Reynolds number, as found in Fig. 13. It says that over the critical Reynolds number, the vortex is shed more frequently and it may bring about a high heat transfer rate on the upper surface of the cylinder as shown in Fig. 2.

3.3. *Discussion*

The side walls of a wind tunnel influence the flow and heat transfer characteristics of bodies tested therein. In the present heat transfer study for the elliptic cylinder, the blockage ratio is the smallest at $\alpha = 0°$, 0.07, and the largest at $\alpha = 90°$, 0.20, respectively. As far as the present authors know, there are no works on the correction rule for the blockage effect upon the heat transfer characteristics of the elliptic cylinder. An attempt, however, has been made to correct such an effect by following the correction formula of Hiwada [22] for the circular cylinder. The correction of Nu_m or Nu_{md} is found to be less than 1% for $\alpha = 0°$ and about 6.6% for $\alpha = 90°$, which is the largest in the present study. Accordingly it may be said that the tunnel wall effect is not severe for the present data.

The critical Reynolds number Re_c found in the heat transfer study is about 44 000 at $\alpha = 15°$ as noted previously. However, measurements of the pressure distribution reveal that it is located at about 90 000. Such a difference of Re_c between the heat transfer and flow measurements may be originated from several factors. First of all, the cylinder tested in the heat transfer study is covered by a stainless steel sheet and then it produces a roughness on the cylinder surface. It is well known that the surface roughness lowers

considerably the critical Reynolds number of the circular cylinder [23]. Furthermore, the tunnel walls also influence Re_c. The increase of the blockage ratio decreases Re_c [24]. These two factors may be most important for the difference of Re_c in the two experiments. However, it may be inferred that the accuracy of the elliptic cylinder has delicate effects upon Re_c. The free stream turbulence intensity and its integral length scale are also factors for such differences in Re_c.

The pressure drag coefficient of a circular cylinder C_{Dd} based on its diameter is 1.1–1.2 in the subcritical Reynolds number region [23]. On the other hand, C_{Dd} of the present elliptic cylinder based on the equivalent diameter d changes from 0.17 at $\alpha = 0°$ to 2.57 at $\alpha = 90°$. An increasing rate of C_{Dd} or C_D with α, however, is not large at small angles of attack, say $\alpha < 20°$, as shown in Fig. 7. In consideration of these facts along with the present data on the mean heat transfer coefficient demonstrated previously, the elliptic cylinder of axis ratio 1 : 3 examined in the present study may be said to have a higher heat transfer ability and a lower fluid dynamic drag compared to the circular cylinder, when the elliptic cylinder is operated at a relatively low angle of attack, say $\alpha < 20°$.

4. CONCLUDING REMARKS

Heat transfer and flow characteristics of an elliptic cylinder having an axis ratio 1 : 3 are clarified through wind tunnel experiments. The Reynolds number range examined is from about 8000 to 79 000, and the angle of attack is varied from 0° to 90°.

The local heat transfer features are quite different from those of a circular cylinder. It is found that the critical Reynolds number exists, over which the heat transfer behaviors change drastically and its value varies with the angle of attack. The correlations between those heat transfer characteristics and the flow around the cylinder are made clear through measurements of the static pressure on the cylinder surface and also of the mean and turbulent fluctuating velocities in the near wake.

The dependency of the mean heat transfer coefficient upon the angle of attack and the Reynolds number is clearly represented. Nu_m is a maximum at $\alpha = 60°$–$90°$, and a minimum at $\alpha = 0°$–$30°$ at low Reynolds numbers but at $\alpha = 20°$–$30°$ at high Reynolds numbers. However, even the minimum value of Nu_m for the elliptic cylinder is still higher than that for the circular cylinder of equal circumferential length. Furthermore, the pressure drag coefficient of the former is lower than that of the latter, say about 1/3 to 1/7 in the region of $\alpha < 20°$. Therefore, the elliptic cylinder of axis ratio 1 : 3 exhibits a superior feature of higher heat transfer capability and lower fluid dynamic drag than the circular cylinder, when the elliptic cylinder is operated at a small angle of attack.

Effects of the axis ratio of the elliptic cylinder upon its mean heat transfer ability are also investigated through a comparison with previous results for a circular cylinder and an elliptic cylinder of different axis ratio. It reveals that an increase of the ratio a/b promotes the heat transfer ability at least in the range $1 \leqslant a/b \leqslant 3$.

Acknowledgements—The authors are grateful to the assistances of Mr N. Kon and also our former students Messrs Y. Kaido, S. Koyama, O. Arai and S. Tomoya in the experiments.

REFERENCES

1. G. B. Schubauer, Air flow in a separating laminar boundary layer, *NACA Rep.* 527 (1935).
2. G. B. Schubauer, Air flow in the boundary layer of an elliptic cylinder, *NACA Rep.* 652 (1939).
3. S. F. Hoerner, *Fluid-dynamic Drag.* Published by the author (1958).
4. V. J. Modi and E. Wiland, Unsteady aerodynamics of stationary elliptic cylinders in subcritical flow, *AIAA J.* **8,** 1814–1821 (1970).
5. V. J. Modi and A. K. Dikshit, Mean aerodynamics of stationary elliptic cylinders in subcritical flow, *Proc. 3rd Int. Conf., Wind Effects on Buildings and Structures*, pp. 345–355 (1971)
6. V. J. Modi and A. K. Dikshit, Near wakes of elliptic cylinders in subcritical flow, *AIAA J.* **13,** 490–497 (1975).
7. S. Taneda, Visual study of unsteady separated flows around bodies, *Prog. Aerospace Sci.* **17,** 287–348 (1977).
8. E. Eckert, Die Berechnung des Wärmeübergangs in der laminaren Grenzschicht umströmter Körper, *VDI ForschHft.* **13**(416), 1–44 (1942).
9. B. T. Chao and R. O. Fagbenle, On Merk's method of calculating boundary layer transfer, *Int. J. Heat Mass Transfer* **17,** 223–240 (1974).
10. R. A. Seban and R. M. Drake, Local heat-transfer coefficients on the surface of an elliptic cylinder in a high-speed air stream, *Trans. Am. Soc. Mech. Engrs* **75,** 235–240 (1953).
11. R. M. Drake, Jr., R. A. Seban, D. L. Doughty and S. Levy, Local heat-transfer coefficients on surface of an elliptic cylinder, axis ratio 1 : 3, in a high-speed air stream, *Trans. Am. Soc. Mech. Engrs* **75,** 1291–1302 (1953).
12. H. Reiher, *Handbuch der Experimentalphysik*, 9–1, 312 (1925).
13. T. Ota, S. Aiba, T. Tsuruta and M. Kaga, Forced convection heat transfer from an elliptic cylinder of axis ratio 1 : 2, *Bull. J.S.M.E.* **26,** 262 267 (1983).
14. R. Hilpert, Wärmeabgabe von geheizten Drähten und Rohren im Luftstrom, *Forsch. Geb. IngWes.* **4,** 215–224 (1933).
15. T. Ota and N. Kon, Heat transfer in an axisymmetric separated and reattached flow over a longitudinal blunt circular cylinder, *Trans. Am. Soc. Mech. Engrs*, Series C, *J. Heat Transfer* **99,** 155–157 (1977).
16. T. Ota, N. Kon, S. Hatakeyama and S. Sato, Measurements of turbulent shear stress and heat flux in an axisymmetric separated and reattached flow over a longitudinal blunt circular cylinder, *Bull. J.S.M.E.* **23,** 1639–1645 (1980).
17. T. Ota and M. Itasaka, A separated and reattached flow on a blunt flat plate, *J. Fluids Engng* **98,** 79–86 (1976).
18. I. Tani, Low-speed flows involving bubble separations, *Prog. Aeronaut. Sci.* **5,** 70–103 (1964).
19. E. Achenbach, Distribution of local pressure and skin friction around a circular cylinder in cross-flow up to $Re = 5 \times 10^6$, *J. Fluid Mech.* **34,** 625–639 (1968).
20. E. Achenbach, Total and local heat transfer from a smooth circular cylinder in cross-flow at high Reynolds number, *Int. J. Heat Mass Transfer* **18,** 1387–1396 (1975).

21. V. T. Morgan, The overall convective heat transfer from smooth circular cylinders, *Adv. Heat Transfer* **11,** 199–264 (1975).
22. M. Hiwada, K. Niwa, I. Mabuchi and M. Kumada, Effects of tunnel blockage on local mass transfer from a column cylinder in cross flow, *Trans. J.S.M.E.* **42,** 2481–2491 (1976).
23. A. Fage and J. H. Warsap, The effect of turbulence and surface roughness on the drag of a circular cylinder, *ARC R&M* 1283 (1930).
24. A. Richter and E. Naudascher, Fluctuating forces on a rigid circular cylinder in confined flow, *J. Fluid Mech.* **78,** 561–576 (1976).

TRANSFERT THERMIQUE ET ECOULEMENT AUTOUR D'UN CYLINDRE ELLIPTIQUE

Résumé—Les caractéristiques du transfert thermique et le comportement de l'écoulement sont clarifiés pour un cylindre elliptique de rapport d'axe 1 : 30. Le fluide étudié est l'air et le nombre de Reynolds varie entre 8000 environ et 79 000. L'angle d'attaque α varie de 0° à 90°. Les allures de transfert thermique locaux et globaux sont comprises en relation avec les structures de l'écoulement autour du cylindre. Le nombre de Reynolds est décelé, et pour lequel les caractéristiques de convection et d'écoulement changent fortement. On trouve que le coefficient de transfert moyen est le plus fort à $\alpha = 60°$–$90°$ pour tout le domaine de Reynolds étudié et aussi que la plus faible valeur de transfert thermique est plus élevée que celle pour un cylindre circulaire. On discute aussi des effets du rapport des axes de l'ellipse, en comparaison avec des travaux antérieurs.

WÄRMEÜBERGANG UND STRÖMUNG IN DER UMGEBUNG EINES ELLIPTISCHEN ZYLINDERS

Zusammenfassung—Das Verhalten von Wärmeübergang und Strömung in der Umgebung eines elliptischen Zylinders mit einem Achsenverhältnis von 1 : 3 wird dargestellt. Das bei den Untersuchungen verwendete Fluid war Luft. Die Reynolds-Zahl lag im Bereich von 8000 bis 79 000. Der Anströmwinkel α wurde von 0° bis 90° variiert. Der örtliche und der mittlere Wärmeübergang wird abhängig vom Strömungsverhalten um den Zylinder beschrieben. Es wird die kritische Reynolds-Zahl bestimmt, bei der sich das Verhalten von Wärmeübergang und Strömung stark ändern. Der mittlere Wärmeübergangskoeffizient hat seinen Höchstwert bei $\alpha = 60°$ bis 90° über den gesamten untersuchten Reynolds-Zahl-Bereich. Der kleinste Wert des mittleren Wärmeübergangskoeffizienten ist sogar noch größer als für einen Kreiszylinder. Einflüsse des Achsenverhältnisses des elliptischen Zylinders werden im Vergleich mit früheren Arbeiten diskutiert.

ТЕПЛООБМЕН И ГИДРОДИНАМИКА ПРИ ОБТЕКАНИИ ЭЛЛИПТИЧЕСКОГО ЦИЛИНДРА

Аннотация—Определены характеристики теплопереноса и течения для эллиптического цилиндра с отношением осей 1 : 30. Исследования проводились с воздухом в диапазоне чисел Рейнольдса от 8000 до 79 000. Угол наклона цилиндра α изменялся от 0 до 90 . Характеристики локального и суммарного теплопереноса определялись в зависимости от режима обтекания цилиндра. Найдено критическое число Рейнольдса, при котором происходит резкое изменение параметров теплопереноса и течения. Установлено, что во всем исследуемом диапазоне чисел Рейнольдса при $\alpha = 60$–90 средний коэффициент теплопереноса достигает наибольшего значения, а также, что даже наименьшее значение средней интенсивности теплопереноса оказывается выше соответствующего значения для случая обтекания круглого цилиндра. Обсуждается роль отношения осей эллиптического цилиндра в рассматриваемых процессах и проводится сравнение с результатами других работ.